Application Note AN-14a
Copyright August, 2003

UWB Signal Sources, Antennas & Propagation

James R. Andrews, Ph.D.
IEEE Fellow & PSPL Founder
Picosecond Pulse Labs, Boulder, Colorado, USA
jrandrews@picosecond.com

Preprint of oral paper to be presented at 2003 IEEE Topical Conference on Wireless Communication Technology, Honolulu, Hawaii, Oct. 15-17, 2003.
Conf. proceedings available only on CD and only contain 2 page summary papers

ABSTRACT: This paper discusses the history of Ultra-Wide-Band (UWB) wireless and considers spectrum issues. It deals with UWB signal sources, including step, impulse, monocycle and rf pulses. It introduces new NLTL technology that can generate 6 V, 4 ps pulses and that can be used for 10 Gb/s, millimeter wave, UWB wireless LANs. Several UWB antennas are presented including: conical, TEM horn, D*dot, monopole and wave guide horn. Experimental proof is given that UWB free space propagation is not wavelength dependent. Sixteen references are included.

UWB HISTORY: Worldwide interest in Ultra-Wide-Band (UWB) wireless has increased greatly with the release in Feb., 2002 by the FCC of their first authorization for UWB [1,2]. UWB is usually considered to be wireless communication or remote sensing using non-sinusoidal carriers, or sinusoidal carriers of only a few cycles duration. While UWB is the current, popular acronym, literature searches on this subject should also include such key words as: impulse radar, Harmuth orthogonal functions, carrier-free, non-sinusoidal, baseband, video pulse, GPR, etc. The FCC's definition of an UWB device is any device whose emissions have a fractional bandwidth greater than 0.2 or occupy >1.5 GHz of spectrum [2]. The early history of UWB really dates back 100 years to the birth of radio. The earliest spark gap transmitters were in reality spark generated impulse excitation of a resonant antenna. Radar as developed in the 1940s, typically used microsecond pulse modulation of a microwave sine wave, and thus had a very low fractional bandwidth. As such, classical radar is not considered to be UWB. The more current history of UWB dates to the 60s & 70s with pioneering work done by Dr. Gerald Ross at the Sperry Research Center and Dr. H.F. Harmuth at Catholic Univ. A good history of the advances during this period is found in E.K. Miller's book [3]. Another good, more recent book is J.D. Taylor's on UWB Radar [4].

UWB SPECTRUM ISSUES: A detailed knowledge is required of the spectrum of the UWB source and also the effect of the radiating antenna on the resultant emitted spectrum. In the FCC's approval of UWB, they placed restrictions on the allowed UWB emission spectrums. For ground penetrating radar (GPR) they required that emissions be below 960 MHz. For most other applications, they required emissions remain within a -10 dB bandwidth from 3.1 to 10.6 GHz. They had particular concerns about interference to GPS systems. For UWB vehicular radar, the FCC restricted the -10dB bandwidth to 22-29 GHz. As part of the FCC UWB study, they received input from NTIA. NTIA's position was "We would also like to draw the attention of UWB developers to the availability of several frequency bands above 40 GHz where some of these types of systems could be operated in conformity with the applicable allocations." [5] Although the FCC did not mention specifically the use of millimeter frequencies in its first UWB report, it did state " ... we intend to review the standards for UWB devices and issue a further rule making to explore more flexible technical standards and to address the operation of additional types of UWB operations and technology" [2]. Thus it would appear that there might be more opportunities for UWB operations at the higher GHz, millimeter frequencies.

UWB SOURCES: The most common electrical signals used to drive UWB antennas include steps, impulses, and mono-cycles [6]. Knowledge of the spectral content of each type of signal is important in determining the amount of filtering required to meet FCC requirements. A step-like pulse has a large amount of spectral energy at low frequencies with the spectrum falling off as 1/f. A narrow, impulsive-like pulse has a flat spectrum of $S_o = V_{pk} * T_d$, i.e. the area of the pulse, where V_{pk} is the peak amplitude and T_d is the 50% duration. The high frequency content of either the step-like or impulse-like pulse is limited by the speed of the transitions involved, either the step risetime, T_r, or the impulse duration, T_d. For ideal waveforms, the first null, f_o, in the spectrum occurs at $1/T_r$ (step) or $1/T_d$ (impulse). Beyond f_o, the spectral content of these pulses die rapidly and typically follow an equation of the form $(\sin(X)/X)^n$. The most important conclusion to be drawn is that generating UWB frequencies in the microwave or GHz range requires pulse transitions in the ultra-fast, picosecond domain. For ground penetrating radar (GPR) in which the spectrum must be contained below 1 GHz, pulse durations must be > ½ ns. For operation in the 3.1-10.6 GHz UWB band, pulse durations (or risetimes) need to be of the order of 50-100 ps. To achieve a reasonably flat spectrum to the millimeter wave region beyond 50 GHz requires a risetime or impulse duration of 10 ps or less.

A monocycle or narrow RF pulse will conserve spectrum and come closer to meeting the FCC spectrum requirements. The spectrum of such a signal can be analyzed as pulse AM modulation of an rf sine wave carrier. The spectrum of the baseband modulating pulse is thus shifted upwards in frequency and centered on the carrier frequency. For rectangular pulse modulation, the spectrum has the classical sin(X)/X shape on each side of the carrier with the first nulls occurring at $f_c + 1/T_d$ & $f_c - 1/T_d$.

To generate these various waveforms, one normally starts with a very fast risetime edge, step-like pulse. To obtain an impulse, one then takes the first derivative of the step risetime. To obtain a monocycle, one takes the first derivative of an impulse or the second derivative of a step. To obtain a narrow rf pulse of a few cycles duration, the technique often used is to "shock excite" a band-pass filter with either a fast rise step pulse or a narrow impulse. If the UWB antenna is appropriately designed, it can function as the band-pass filter. If insufficient power is obtained from these elementary generating methods, then a wideband post amplifier is required.

To obtain GPR pulses of > 1/2 ns to a few ns duration, various high power switching transistors or FETs can be used. Avalanche transistors are often used and they can generate peak power levels from 50 watts to several kilowatts. For the 3-10 GHz UWB band, the selection of available devices is much smaller. Step Recovery Diodes (SRDs) have been used for many years to generate 50 - 200 ps edges with amplitudes of several volts. There are now also available some FETs and logic ICs which were developed for 5-10 Gb/s fiber optic applications which produce 1 V_{ptp} differential pulses with 50-100 ps edges.

To achieve < 10 ps edges to reach out to the millimeter range, the choices are very limited. One new promising technology that is just now becoming commercially available is the Non-Linear Transmission Line (NLTL) Edge Compressor [7,8]. NLTLs can be driven over extremely wide data rates from kbits/s to beyond 12 Gb/sec. Thus they offer the potential of creating 10 Gb/s, millimeter, UWB, local area wireless networks. An NLTL is a synthetic transmission line [9] consisting of series inductors and shunt voltage variable capacitors provided by varactor diodes, Fig. 1. The time delay through the NLTL is a function of the signal amplitude. For the diode polarity shown in Fig. 1, and a positive polarity input pulse, the lower voltage portions of the pulse are delayed more than higher voltages. This has the net effect of compressing the rising edge to a faster risetime, Fig. 2. The opposite effect is produced on the trailing, falling edge of the pulse. Fig. 3 shows a 6 Volt, 4 ps risetime pulse generated by a commercial NLTL.

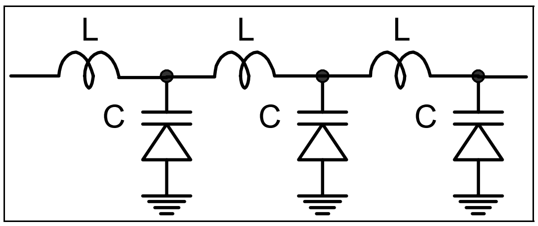

Fig. 1 Non-Linear Transmission Line Schematic

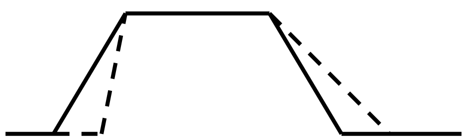

Fig. 2 Input & output (---) pulses for a positive polarity NLTL.

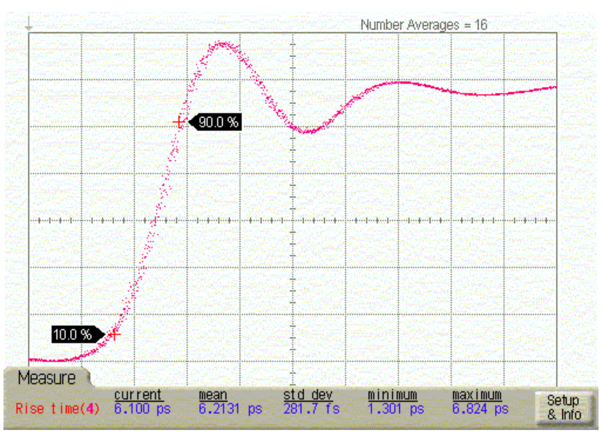

Fig. 3 6 Volt, 4 ps risetime pulse from PSPL NLTL pulse gen. as measured by PSPL 100 GHz sampling oscilloscope. 1 V/div & 5 ps/div.

UWB ANTENNAS: There are almost no companies selling commercial UWB antennas. One exception is Farr Research, in Albuquerque, NM, www.farr-research.com. However, since the early 1970s there exists in the technical literature a very large quantity of papers on UWB antennas. Much of the early pioneering work on UWB antennas was done at NBS [10, 11] and in the military EMP community. Perhaps the largest body of published work is in the Air Force Research Labs collections [12], edited by Dr. Carl Baum.

A very important but frequently overlooked concept about UWB antennas is that the commonly accepted principle of antenna transmit-receive reciprocity does not exactly hold true for their time domain performance. Dr. Motohisa Kanda, of NBS, has shown "that the transmitting transient response of an antenna is proportional to the time derivative of the receiving transient response of the same antenna" [11]. His derivation in section 5.1 in ref. [11] shows that there is an extra "jω" factor in the antenna reciprocity relationship. For engineers working in the frequency domain at a single frequency, or a narrow band of frequencies, this "jω" term simply amounts to a 90-degree phase shift term, i.e converts the frequency domain sine wave into a cosine wave. Thus it has been ignored in the classical frequency domain antenna design and everyone has assumed that an antenna's gain is identical for either transmitting or receiving. In the time domain, however, this "jω" term has a dramatically different effect of either differentiating or integrating, depending upon the usage of an antenna.

For metrology purposes, the antennas recommended by NIST are the conical antenna for transmission and the TEM horn for reception. The conical antenna radiates an E-M field that is identical in waveform to the voltage driving the antenna. The TEM horn antenna outputs a voltage waveform that is identical to the incident E field. Another receiving antenna that is also used for metrology purposes is the D*dot probe. Its voltage output is the first derivative of the incident E field.

A miniature UWB antenna range, Fig. 4, was designed to demonstrate the principles of UWB transmission, reception and propagation. The UWB metrology antennas demonstrated on this range include the conical, TEM horn and D*dot

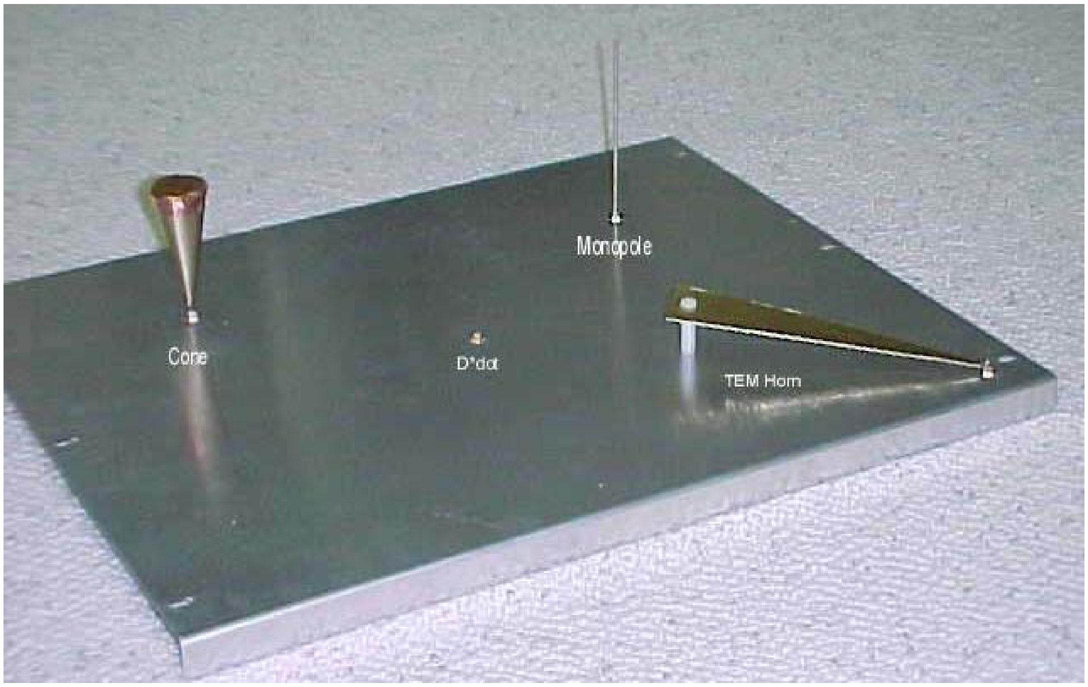

Fig. 4 Miniature UWB Antenna Range. Antennas shown include a conical antenna, TEM Horn antenna, D*dot probe antenna and a Vertical Monopole Antenna.

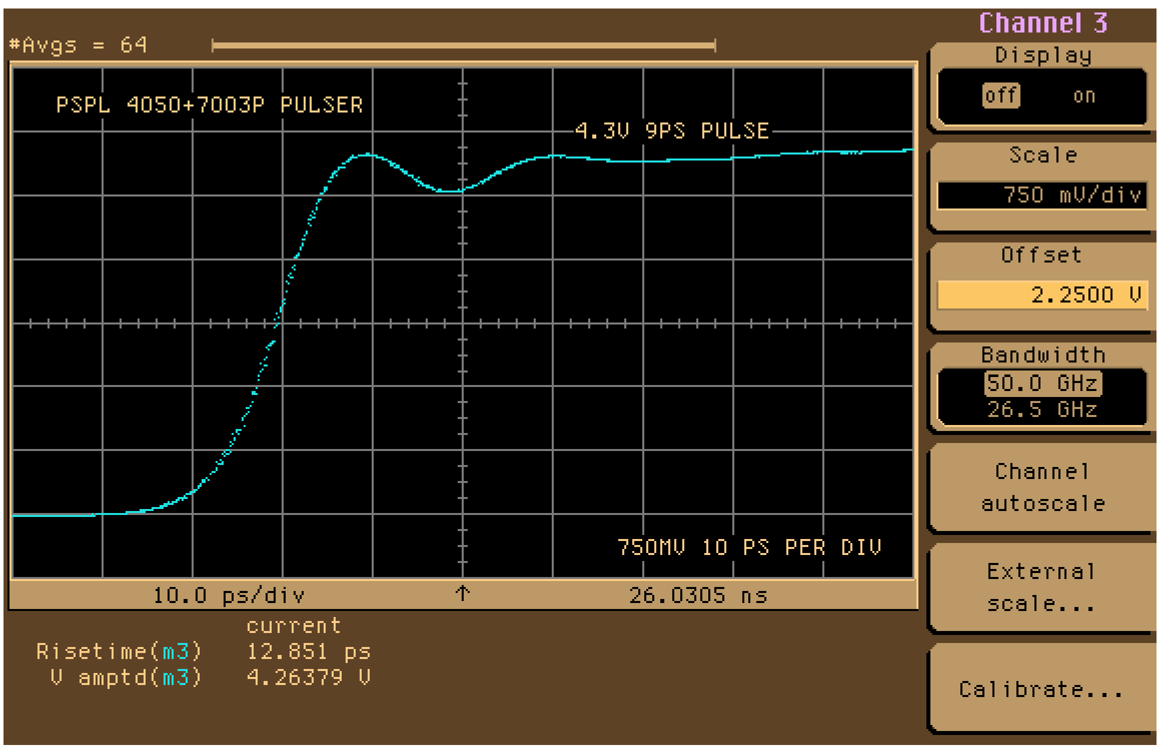

Fig. 5 4 Volt, 9 ps risetime, step pulse used for UWB antenna testing. Measured by an HP 50 GHz, 9 ps risetime, sampling oscilloscope. Scales are 750mV/div & 10 ps/div.

probe. Monopole antennas and wave-guide horn antennas were also studied. Both differentiation and integration effects in the time domain will be demonstrated by these various antennas. Construction details for the antenna range and the antennas are found at the end of this paper. The ultra-broadband test input signal used on this antenna range was a 4 V, 9 ps risetime step pulse from an NLTL pulse source, Fig. 5. With the conical transmitting antenna, the incident E field, E_{inc}, onto the various test antennas is a close replica of this waveform. All of the waveforms shown in this paper were measured using a HP-54752B, 50 GHz, 9 ps risetime oscilloscope. A 35 cm, Gore, SMA coaxial cable was used to connect the antennas to the oscilloscope. The risetime of this cable was 9 ps. Thus the composite risetime of the pulse generator, coax cable and oscilloscope was 16 ps.

CONICAL ANTENNA: The conical antenna suspended over a large metal ground plane is the preferred antenna for transmitting known transient electro-magnetic waves. This type of antenna is used by NIST as their reference standard transient transmitting antenna [13]. This antenna radiates an E-M field that is a perfect replica of the driving point voltage waveform. This antenna can be analyzed as one half of the bi-conical transmission line [14] with a uniform characteristic impedance given by

$$Z_{cone} = (\eta / 2\pi) * \ln[\cot(\theta_o/2)] \qquad (1)$$

where η is the free space impedance of 377 Ω and θ_o is the solid ½ angle of the cone. A 4° cone has a 200 Ω impedance, while a 47° cone is required to achieve a 50 Ω impedance. The electric E field generated at radius, *r*, and angle, θ, is given by

$$E_\theta(r,t) = V_{base}(t-r/c) / \{r * \sin(\theta) * \ln[\cot(\theta_o/2)]\}$$

$$\text{valid only for } t < l/c \qquad (2)$$

The driving point voltage at the base of the conical antenna is given by

$$V_{base}(t) = V_{gen}(t) * R_{cone} / (R_{cone} + R_{gen}) \qquad (3)$$

An important point to remember when using the conical antenna is that eqn. 2 is only valid for the time window up to $T_w = l / c$, where *l* is the length of the antenna. For $t > T_w$, the original incident wave launched on the antenna has reached the end of the antenna and is reflected, thus setting up a series of multiple reflections on the antenna radiating element. The radiated E field is thus no longer a replica of the driving point voltage, but is now corrupted by the multiple reflections. Practical UWB conical antennas will include resistive loading on the far end of the antenna to help suppress multiple reflections. The upper bandwidth of a conical antenna is mainly determined by the fidelity of the coax connector to conical antenna transition region. If a conical antenna is used as a receiving antenna, its output is the integral of the incident E field.

TEM HORN ANTENNA: TEM horns are the most preferred metrology receiving antenna for making a direct measurement of transient E-M fields. The TEM horn antenna is basically an open-ended parallel plate transmission line. It is typically built using a taper from a large aperture at the receiving input down to a small aperture at the coax connector output. The height to width ratio of the parallel plate is maintained constant along the length of the antenna to maintain a uniform characteristic impedance, R_{ant}. The output from a TEM antenna is

$$V_{out}(t) = h_{eff} * E_{inc}(t) * R_{load} / (R_{ant} + R_{load}) \qquad (4)$$

where h_{eff} is the effective height at the aperture of the antenna. This equation is only valid for times less than twice the electrical length of the antenna. Ideally to suppress multiple reflections, the antenna impedance should match the 50 Ω output cable. However, to optimize sensitivity, most TEM antennas are designed with a 100 Ω antenna impedance. Practical UWB TEM horn antennas are usually designed with resistive loading near the mouth of the antenna to help suppress multiple reflections. The upper bandwidth of a TEM antenna is mainly determined by the size of its aperature and secondarily by the parallel plate to coax connector transition. When the aperture is too large relative to the wavelength of incident fields, the parallel plate line becomes a waveguide with higher order TE and TM modes present which in turn limit its bandwidth. If a TEM antenna is used as a transmit antenna, the radiated E field is the first derivative of the input driving point voltage.

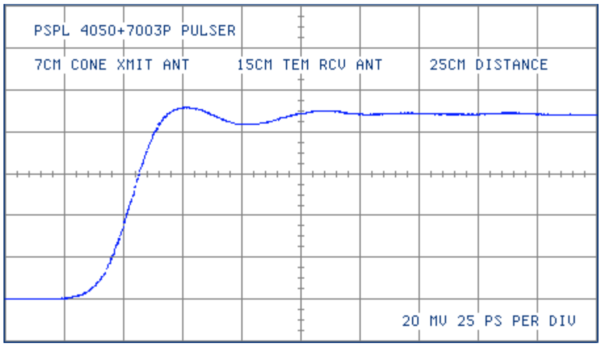

Fig. 6 Transmission from a conical antenna to a TEM horn antenna over a 25 cm path.

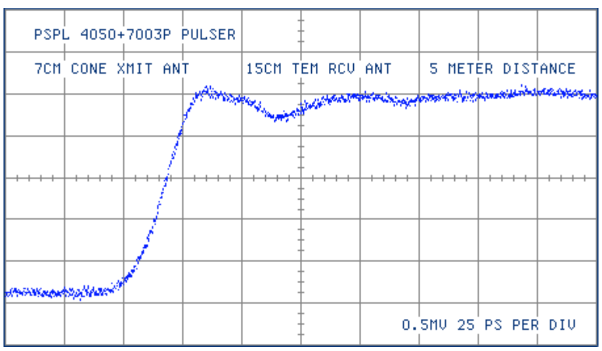

Fig. 7 Transmission from a conical antenna to a TEM horn antenna over 5 meter path.

UWB CONE - TEM ANT. EXPERIMENTAL RESULTS: To demonstrate faithful UWB radiation and propagation the conical antenna and TEM horn shown on the test range, Fig. 4, were used. The 4 V, 9 ps rise pulse, Fig. 5, was connected directly to the conical antenna. The output of the TEM horn antenna was connected through the 35cm cable to the 50 GHz oscilloscope. The conical antenna was 7 cm high and had an impedance of 132 Ω. The TEM horn was 15 cm long and had an impedance of 106 Ω. For most of the experimental data shown in this paper, the separation between the antennas was 25 cm. Fig. 6 is the output of the TEM horn antenna. This shows a 23 ps risetime step waveform that is in good agreement with the input waveform, Fig. 5. Fig. 7 shows the output from the TEM horn antenna when the two antennas were separated by 5 meters. This received signal is identical in wave shape to the 25 cm path, Fig. 6, except that it is weaker in amplitude. Fig. 8 shows the received waveform when transmitting a step E-M field between a pair of identical conical antennas. The resultant received output, rising ramp, waveform is the integral of the generator's step pulse. This illustrates that a conical receive antenna integrates the incident E field. Fig. 9 shows the received waveform when using a pair of identical TEM horn antennas for transmit and receive. The resultant output, impulse, waveform is the first derivative of the pulse generator's step pulse. This illustrates that a TEM horn transmit antenna radiates an E field which is the first derivative of the signal generator's waveform.

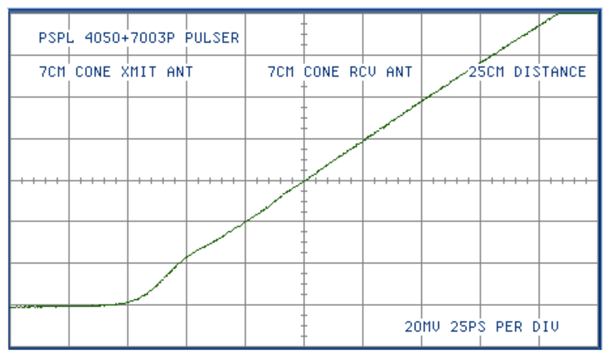

Fig. 8 Transmission between a pair of identical conical antennas.

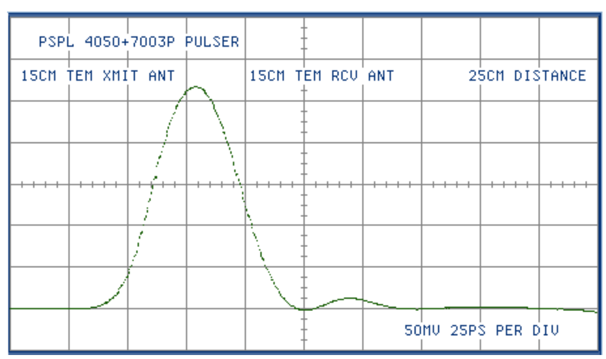

Fig. 9 Transmission between a pair of identical TEM horn antennas.

UWB PROPAGATION: Classical radio theory [15] states that the free space path loss is a function of wavelength and is given by the following equation:

$$\text{Path Loss (classical)} = (4\pi * r / \lambda)^2 \qquad (5)$$
$$\text{or in dB} = 20 * \log(4\pi * r / \lambda)$$

where r is the path distance between antennas and λ is the wavelength.

"It is a common misconception that free space propagation is wavelength dependent." [16] The reason for this misconception is the underlying assumption in radio engineering text books that one is calculating the loss at a specific frequency between two isotropic antennas or $\lambda/2$ dipoles. The voltage induced into an antenna is

$$V_{ant} = h_{eff} * E_{inc}. \qquad (6)$$

For $\lambda/2$ dipoles, the effective height, h_{eff} , is directly proportional to the wavelength. Thus the received power is in fact reduced as the wavelength decreases, but the loss is not in the path, but rather due to the fact that a shorter antenna is being used. The above path loss equation (5) works fine for people working solely in the frequency domain with narrow band antennas. However, for time domain, UWB signals, this equation conveys false information. When dealing with UWB signals, the path loss should really be considered not for the output voltage from an antenna, but rather for the Poynting Vector, Power Density, P_d in Watts/ m^2 or the E field in Volts/m incident upon the receiving antenna,

$$P_d = E^2 / \eta \qquad (7)$$

where η is the free space impedance of 377 Ω. From this perspective, the path loss then is due solely to the spherical geometry of an expanding wave emanating from a point source at the center of the sphere. Recall that the total radiated power is equal to the spherical integration of the Poynting vector over the whole surface of the sphere. Thus the path loss equation should instead be simply the ratio of a unit area of 1 m^2 to the total surface area of a sphere of radius r (in meters).

$$\text{Path Loss (in dB)} = 10*\log[(1\ m^2) / (4\pi r^2)] \qquad (8)$$
$$= -11\text{dB} - 20*\log(r)$$

Experiments were performed at various antenna separations to verify that the path loss theory of eqn. (8) was valid. The experiments showed that the strength of the radiated E field was in fact inversely proportional to the path distance, r.

Another argument against including a wavelength factor in the path loss is --- if the path loss were really in fact a function of wavelength (i.e. spectrum), then the higher frequencies in a radiated UWB signal would be severely attenuated and the received waveform would be grossly distorted and smeared out from the transmitted waveform. That is not the case at all. Figs. 6 & 7 showed the identical received signals at the TEM horn antenna over both a 25 cm and 5 meter paths. These waveforms are identical in shape to those of the signal generator and are only attenuated in amplitude as a function of the path length. When driven by the step-like voltage waveform, the conical antenna radiated a step-like E field, which in turn induced a step-like voltage waveform into the TEM horn antenna. The only risetime/frequency limitations were the finite bandwidths of the antennas and not the intermediate free-space path loss.

OTHER ANTENNA EXPERIMENTS: The remainder of this paper will demonstrate the UWB performance of several other antennas. They include the D*dot, monopole, and waveguide horn antennas.

D*dot PROBE ANTENNA: The D*dot antenna is another popular UWB metrology antenna. The D*dot antenna is basically an extremely short, monopole antenna [14]. The equivalent antenna circuit consists of a series capacitance and a voltage generator, $V_{ant,}$ given by eqn. (6) above. For a very short monopole, the antenna capacitance is very small and the capacitor thus acts like a differentiator to transient E-M fields. Therefore the output from a D*dot probe antenna is the first derivative of the incident E field. To determine the actual wave shape of the incident E field, one must integrate the output from the D*dot probe. When the frequencies become too high, the D*dot probe loses its derivative properties and it becomes a monopole antenna. This happens when the length of the D*dot probe approaches a quarter wavelength of the incident wave.

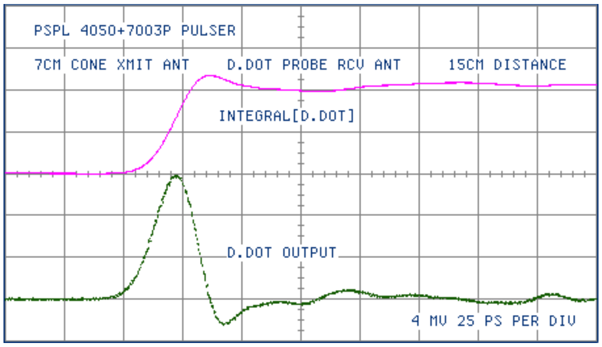

Fig. 10 Transmission from conical antenna to D*dot antenna. The lower trace is the output from the receive antenna. The upper trace is the integral of the lower trace.

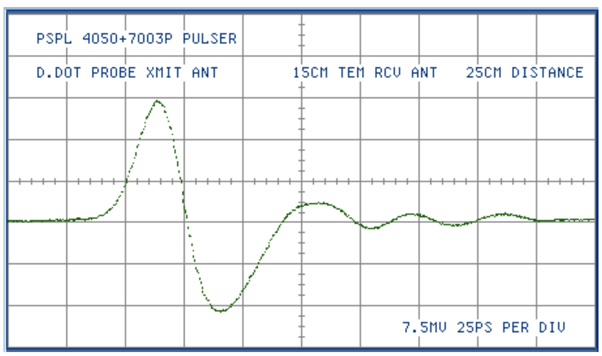

Fig. 11 Transmission from a D*dot antenna to a TEM horn antenna.

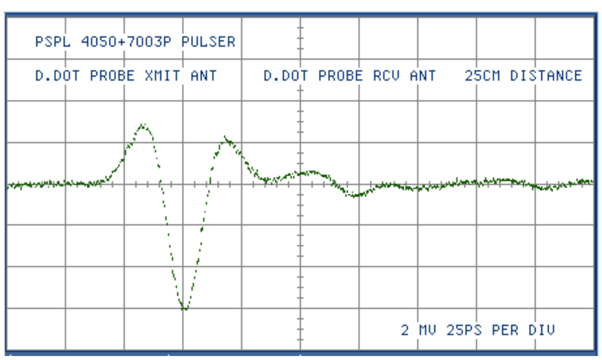

Fig. 12 Transmission between a pair of identical D*dot antennas.

Fig. 10 is the output from a D*dot receive antenna when it was illuminated with a step E-M field radiated from a conical transmit antenna. The lower trace is the actual receive antenna output. It is a 19 ps wide impulse which is consistent with the antenna's output being the first derivative of E_{inc}. The upper trace is the computed integral of the lower trace. It has a 19 ps risetime step and is a good representation of the incident E field at the antenna. Fig. 11 shows the radiated field from a D*dot transmit antenna. It was received by a TEM horn antenna. This shows that the transmitting transient response of the D*dot antenna is the second derivative of the driving generator voltage. Fig. 12 is the received output signal using a pair of D*dot antennas for both transmit and receive. This signal is the third derivative.

MONOPOLE ANTENNA: A monopole antenna was included in this UWB study, because it is the most fundamental building block antenna for most antenna designs. It is the quarter wave whip antenna above an infinite ground plane. The monopole antenna is sometimes used as a simpler version of the conical antenna for transmitting UWB signals which are similar in wave shape to the driving point voltage. However, its radiated fields are not as uniform as those for the conical antenna. Its driving point impedance is not constant, but rises as a function of time. This leads to distortion of the radiated E-M fields. TDR studies of a monopole confirm this statement. Fig. 13 shows the radiated E field of a 10 cm monopole. It resembles the step E field from the conical antenna, Fig. 6. However its top line is not flat, but sags with increasing time. This is due to the non-uniform TDR impedance of this antenna.

When a monopole is used for receiving transient E-M fields, its output is the integral of the incident E field. This is show experimentally in Fig. 14. The lower trace is the antenna output. It shows an almost monotonically rising ramp which is consistent with the integral of the step incident E field. The upper trace is the calculated first derivative of the lower trace and is somewhat representative of the step E_{inc}. Fig. 15 shows the output using a pair of 10 cm monopoles for both transmit and receive. This is essentially the integral of the generator's step pulse. The integration effect can be explained simply. Assume an impulsive E field is incident upon the monopole at a 90° angle to its axis. Thus a current is induced simultaneously in each differential element, *dx*, of the antenna. These current elements, *di*, thus start to flow towards the output connector of the antenna. They do not arrive at the output simultaneously, but in sequence. Thus the output appears as a step function, which is the integral of the incident impulse. The integrating effect of this antenna only lasts for t < *l* / c, where *l* is the length of the antenna. This effect is demonstrated in Figs. 16 and 17 for a transmitting/receiving pair of shorter 2 cm monopole antennas. Fig. 16 shows the output starts off like a rising linear ramp, as in Fig. 15, but due to the short length of the antenna, this stops after *l* / c = 67 ps and then the multiple reflections on the antennas predominate. This is shown vividly in Fig. 17 on a slower speed of 100 ps/div in which the resonance frequency of the 2 cm antennas is obvious as a damped, ringing, sinusoid.

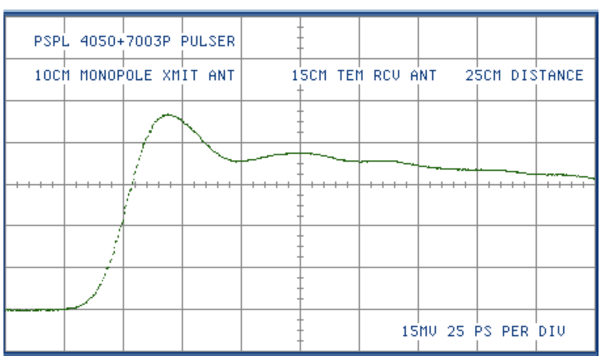

Fig. 13 Transmission from monopole to TEM

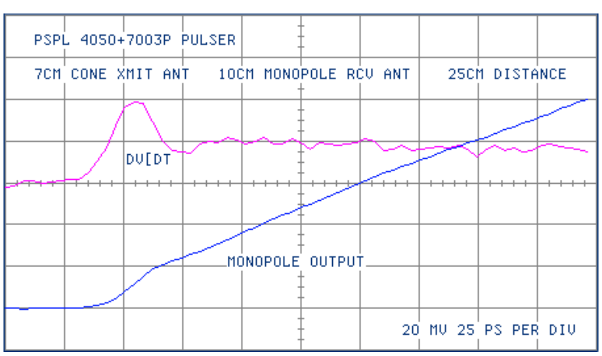

Fig. 14 Transmission from conical to monopole
Lower trace rcv. ant. output. Upper trace is dV/dt

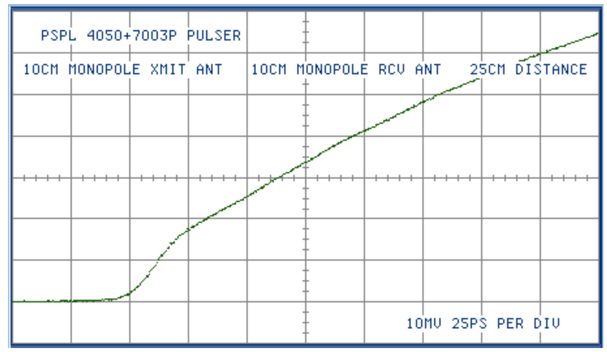

Fig. 15 Transmission between a pair of identical 10 cm monopole antennas.

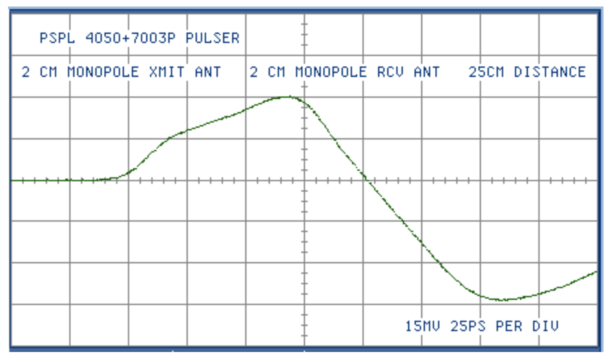

Fig. 16 Transmission between a pair of identical 2 cm monopole antennas. 25 ps/div.

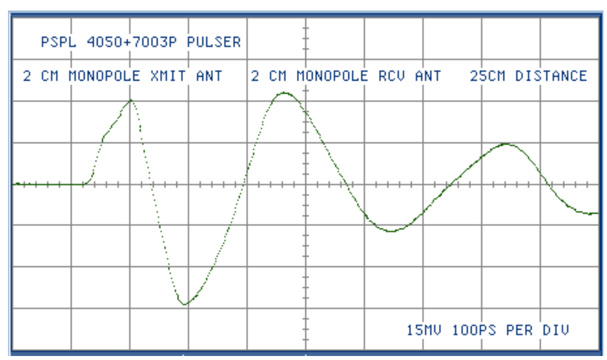

Fig. 17 Transmission between a pair of identical 2 cm monopole antennas. 100 ps/div

GAIN / BANDPASS ANTENNAS: Most practical UWB systems will not in fact use the UWB metrology antennas discussed above. To meet FCC spectrum requirements, considerable band-pass filtering will need to be done. The particular antenna chosen can accomplish this. We present here an example suitable for the FCC 3.1-10.6 GHz UWB band. The antennas used were E-Systems, C-band, wave guide, horn antennas. A network analyzer VSWR test of this antenna showed its pass-band (< 3:1 vswr) covered from 4.7 to 10.1 GHz. Fig. 18 shows the result of using a pair of these C-band horn antennas for both the transmitting and receiving antennas. The transmit antenna was driven by the 4 V, 9 ps pulse, Fig. 5. The antenna separation was 5 meters. The output no longer resembles a step, but is in fact the step response of a band-pass filter, which is a damped, ringing sinusoid. The frequency of the sinusoid is near that of the band-pass filter's center frequency. If the filter is narrow-band, then the sinusoid will ring for many cycles. The wider the band-pass of the filter, the fewer cycles there will be in the sinusoid. The gain of these antennas is now quite apparent compared to the conical / TEM horn combination of Fig. 7. The damped sinusoid has an amplitude of 27 mV_{ptp} versus the 2.4 mV step amplitude.

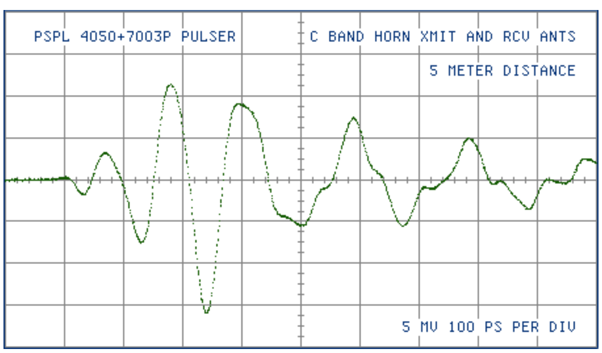

Fig. 18 Transmission between a pair of identical C-band waveguide horn antennas. 5 meter path

ANTENNA DETAILS: The antennas used for this paper are simple to fabricate. The mini-antenna range consisted of an 36 cm x 44 cm aluminum plate. Bulkhead mount SMA jacks (CDI p/n 5110CC) were used for the antenna coax connectors.

For the conical antenna a brass sheet was rolled into a conical shape and soldered onto the SMA connector's extended center conductor. The extended Teflon insulator was not removed. The height of the cone was 7 cm. The cone's ½ solid angle was 12°. A TDR test showed the cone's impedance to be very uniform at 132 Ω.

The TEM horn was fabricated from a 0.015" brass sheet. The overall length was 15 cm. It was supported at the mouth by an 8-32 x 1" nylon spacer with nylon screws. The height at the mouth was 2.6 cm. The width at the mouth was 3.8 cm. The height to width ratio of 0.68 was maintained along the entire length of the antenna. The approximate incline angle was 9°. The tapered end was soldered to the SMA jack's extended center conductor at a height of 1.9 mm. The exposed Teflon on the SMA was removed. A TDR test showed an abrupt TDR jump from 50 Ω at the connector to 106 Ω along the entire length of the antenna. It should be noted that earlier attempts to fabricate this antenna using copper plated, printed circuit boards were not satisfactory. The presence of the p.c. board dielectric material alongside the metal surface leads to phase distortion and resultant slower risetimes.

The D*dot probe antenna is simply an SMA jack with the extended Teflon cut back flush to the mounting nut. To maximize the bandwidth, the length of the jack's exposed center conductor was trimmed back to 1.8 mm. This gave a λ/4 cutoff frequency of 42 GHz.

For the monopole antenna, the extended Teflon dielectric of the SMA was trimmed back flush with the mounting nut. A 10 cm long, 0.1" dia. brass rod was slipped over the connector's extended center conductor and soldered in place. A TDR test of the monopole showed that its impedance varied from 150 Ω at the SMA end to 300 Ω at the far end.

These antennas were all built solely for the purpose of demonstrating the early time properties of UWB signals. Most antennas built for UWB purposes also include in their design resistive loading along the antenna structure. This is done to help suppress the multiple reflections that eventually occur when the antenna is pulsed.

REFERENCES:

[1] FCC News Release, "New Public Safety Applications and Broadband Internet Access Among Uses Envisioned by FCC Authorization of Ultra-Wideband Technology", 14 Feb 2002

[2] FCC 02-48, "Revision of Part 15 of the Commission's Rules Regarding Ultra-Wideband Transmission Systems", First Report & Order, Washington DC, Adopted 14 Feb 2002, Released 22 April 2002.

[3] E.K. Miller, editor, Time-Domain Measurements in Electromagnetics, Van Nostrand Reinhold, New York, 1986

[4] J.D. Taylor, editor, Introduction to Ultra-Wideband Radar Systems, CRC Press, Boca Raton, 1995

[5] W.T. Hatch, NTIA Acting Assoc. Admin, NTIA UWB Position Letter to FCC, attn. D. Hatfield, 15 June 1999.

[6] J.R. Andrews, "Picosecond Pulse Generators for UWB Radars", AN-9, Picosecond Pulse Labs, Boulder, CO, May, 2000

[7] S. Pepper, J.R. Andrews, "Driving & Biasing PSPL Edge Compressor Components", AN-13, Picosecond Pulse Labs, Boulder, CO, Oct, 2002

[8] W. Thomas, R.C. Smith & K. Schoen, "Comb Generator with Excellent Harmonic Flatness to >40 GHz", submitted to MTT-2003.

[9] M. Rodwell, et.al, "GaAs Nonlinear Transmission Lines for Picosecond Pulse Generation and Millimeter Wave Sampling", IEEE Trans. MTT, vol. 39, no. 7, July 1991, pp. 1194-1204

[10] R. Lawton & A. Ondrejka, "Antennas and the Associated Time-Domain Range for the Measurement of Impulsive Fields", Nat. Bur. of Stds. Tech. Note 1008, Boulder, CO, Nov. 1978

[11] Dr. Motohisa Kanda, "Time-Domain Sensors & Radiators", chapter 5 in ref [3]

[12] Dr. Carl Baum, editor, "Sensor & Simulation Notes 1964 - 1998" and "Interaction Notes 1970 - 2001", Air Force Research Labs, Kirtland AFB, NM

[13] R. Johnk & A. Ondrejka, "Time-Domain Calibrations of D-Dot Sensors", NIST Tech. Note 1392, NIST, Boulder, CO, Feb. 1998

[14] S. Ramo & J. Whinnery, Fields & Waves in Modern Radio, J. Wiley, New York, 2ed edition, 1962, pp. 406-408.

[15] R. Hansen, "Antennas", chp. 32, in Reference Data for Engineers: Radio, Electronics, Computer, and Communications, H.W. Sams, Indianapolis, IN, 7^{th} edition, 1985, p. 32-3

[16] D. Dobkin, "Indoor Propagation Issues for Wireless LANs", RF Design, Sept, 2000, pp 40-46.